Viscosity and elastic constants of amorphous Si and Ge

Viscosity and elastic constants of amorphous Si and Ge

Ann Witvrouw[a] and Frans Spaepen
Division of Applied Sciences, Harvard University, Cambridge, Massachusetts 02138

(Received 4 August 1993; accepted for publication 26 August 1993)

The biaxial modulus and coefficient of thermal expansion of ion-beam-sputtered amorphous Si and Ge thin films were determined from curvature changes induced by differential thermal expansion. Viscous flow was measured by stress relaxation and was found to be Newtonian. The viscosity increased linearly with time as a result of structural relaxation, and its isoconfigurational activation enthalpy was 1.8 ± 0.3 and 2.6 ± 1.3 eV for amorphous Si and Ge, respectively. An atomistic model, based on a chain reaction of broken bond rearrangements, is proposed to describe the observation.

I. INTRODUCTION

Silicon and germanium form the simplest covalently bound amorphous solids. Their structure is a continuous random network,[1–3] in which all atoms have four neighbors at the same distance, as in the crystal; the lack of translational symmetry arises from deviations of the bond angle from the ideal tetrahedral value. This simple structure is ideal for the study of plastic flow in the amorphous state in general and of network formers, such as silicates, in particular. That, nevertheless, plastic flow of amorphous Si and Ge has hardly been studied is because they are prepared in thin-film form. The recent surge in interest in the mechanical properties of thin films has led to the development of techniques based on substrate curvature for the measurement of stress relaxation in thin films.[4–7] Plastic flow in amorphous Si was first observed with these techniques during and after ion irradiation.[8] This article reports a study of the viscosity of sputter-deposited samples as a function of stress (to establish the Newtonian character of the flow), temperature, and time from stress relaxation experiments.

The time dependence of the viscosity is characteristic of all amorphous materials, and results from structural relaxation. This phenomenon affects many of their properties. In amorphous Si and Ge changes in enthalpy,[9–11] diffusivity,[12] and optical properties[13–15] have been observed, and the process has been interpreted atomistically as a continuous decrease in the concentration of structural defects.[16–18] It is known that structural relaxation in other covalent network formers, such as silicate glasses, has a strong effect on their viscosity.[19] The same is therefore expected for amorphous Si and Ge.

To obtain absolute values of the viscosity from stress relaxation experiments the biaxial modulus of the films must be known. Only a few determinations of elastic constants of amorphous Si and Ge are reported in the literature.[20–22] Since the moduli may depend on the preparation method and thermal history, the biaxial moduli of the actual films studied here needed to be determined, and this was done by measuring the stress in the films as a function of temperature for films deposited on different substrates.

II. EXPERIMENTAL TECHNIQUES

For biaxial bending of a thin film of thickness d_f on a substrate with thickness d_s ($d_f \ll d_s$), the biaxial stress σ in the film is given by[4,23,24]

$$\sigma=\frac{1}{6}\left(\frac{E_s}{1-\nu_s}\right)\frac{d_s^2}{d_f}K, \tag{1}$$

where E_s and ν_s are Young's modulus and Poisson's ratio of the substrate. This stress relaxes by viscous flow according to the differential equation[25]

$$\frac{\sigma}{6\eta}+\frac{\dot{\sigma}}{E_f/(1-\nu_f)}=0, \tag{2}$$

where $Y_f=E_f/(1-\nu_f)$ is the biaxial modulus of the film and η its instantaneous shear viscosity. Monitoring the curvature of the specimen as a function of time at constant temperature allows the determination of the viscosity if Y_f is known.

Y_f can be determined from measurements of stress versus temperature for films deposited on two different substrates.[26,27] When both the film and substrate have tetragonal or higher symmetry at all temperatures and no plastic flow occurs, the changes in stress σ with temperature T in the film are due to the difference between the coefficients of thermal expansion of the film α_f and the substrate α_s,

$$\sigma=\sigma_0+\frac{E_f}{1-\nu_f}(\alpha_s-\alpha_f)(T-T_0), \tag{3}$$

where σ_0 is the stress at temperature T_0. If the elastic constants and the coefficients of thermal expansion of the substrates are known, at least two equations or two different substrates are needed to solve for the two unknowns: α_f and $E_f/(1-\nu_f)$.

The substrate curvature is measured by reflecting a laser beam from the surface of the specimen and determining its displacement, at a distance of 1 m, as the specimen

[a]Present address: IMEC, Kapeldreef 75, 3001 Leuven, Belgium.

 0021-8979/93/74(12)/7154/8/$6.00

TABLE I. Calculated biaxial moduli and coefficients of thermal expansion for ion-beam-sputtered (a) amorphous Si at an average temperature of 110 °C and (b) amorphous Ge at an average temperature of 172 °C from changes in stress with temperature for thin films deposited on Si(100) and fused quartz substrates.

Substrate	Highest T (°C)	Y_s (10^{10} Pa)	α_s (10^{-6}/K)	$\Delta\sigma/\Delta T$ (MPa/K)	Y_f (10^{10} Pa)	α_f (10^{-6}/K)
			(a) Si			
Si(100)	198	17.95	3.044	$+0.004\pm 0.015$	14 ± 1	3.0 ± 0.3
Fused quartz	198	8.66	0.5	-0.36 ± 0.03		
			(b) Ge			
Si(100)	298	17.88	0.314	-0.57 ± 0.02	12 ± 1	7.9 ± 0.7
Si(100)	322					
Fused quartz	322	8.76	0.505	-0.88 ± 0.02		

is moved. For a sample with a constant radius of curvature R, the slope of the displacement plotted versus specimen position is $2K$ with $K=1/R$ the curvature of the specimen. The construction of the apparatus used for this work has been described previously.[5,28] *In situ* experiments at elevated temperatures were carried out in a small vacuum chamber with a heater and an optically flat window. The chamber was backfilled with titanium-gettered flowing He (99.999%) at a slight overpressure. Titanium pieces were also put on top of the heater as a getter. As a result, no effects ascribable to oxidation were observed. The temperature was kept constant within 1 °C. After stress relaxation at one temperature for several hours, the temperature was raised by 50 or 100 °C and new relaxation data was taken. This could be repeated several times.

Amorphous Si and Ge thin films, approximately 1 μm thick, were ion-beam sputtered[29] from elemental targets onto $1\times 1/4$ in.^{2} Si(100) (about 380 μm thick) fused quartz substrates (about 520 μm thick) and Ge(111) substrates (400 and 450 μm thick). The thickness of the films was determined by channeling in Rutherford backscattering (RBS), using a density that is 1.7% smaller than that of the crystalline material.[30] The curvatures of the substrates were measured before sputtering and were subtracted out. The compressive sputtering stress for the amorphous Si and Ge thin films is, respectively, about 0.9 and 0.3 GPa.

The exact thickness of the substrates was determined by a 1000 point thickness measurement across each 3 in. wafer for the Si substrates (performed by the supplier, the ZITI corporation) and by a 5 point micrometer measurement for the other substrates.

III. RESULTS

A. Elastic constants

The biaxial moduli Y_f of amorphous Si and Ge thin films were determined by measuring the stress in the films as a function of temperature for films deposited on Si(100) and fused quartz substrates. In order to eliminate viscous flow during the measurements, they were made during the cooldown of a series of consecutive viscous flow runs for several hours at 149 and 199 °C for amorphous Si and at 152, 200, 249, and 298 °C or 126, 176, 225, 274, and 323 °C for amorphous Ge. The results for $\Delta\sigma/\Delta T$ are presented in Table I. From these data on both substrates the biaxial modulus Y_f and the coefficient of thermal expansion α_f of each material were determined using Eq. (3). Their values are listed in Table I. For amorphous Ge on Si(100) the average $\Delta\sigma/\Delta T$ value from the two experiments was used. The values of the biaxial moduli Y_s and coefficients of thermal expansion α_s of the substrates used in Eq. (3) are the averages of the values for the highest and the lowest temperature (room temperature) of the sample during the experiment.[31–34] These values are also listed in Table I.

The values of Y_f for amorphous Si and Ge are, respectively, 79% and 86% of the {100} crystalline value at the same average temperature.[31,32] The values for amorphous Si agree with the literature value of 15×10^{10} Pa (Refs. 21 and 22) for hydrogenated amorphous Si with a small amount of hydrogen. Bhadra *et al.*[20] measured the surface wave velocity, v in Si(100) during amorphization by ion bombardment and its value changed from 4.8 to 4.15 km/s. Since v^2 is proportional to E/ρ, a decrease in the density ρ of 1.7%,[30] and an assumed constant Poisson's ratio ν, gives $E/(1-\nu)=13.3\times 10^{10}$ Pa for implanted amorphous Si, close to the value measured here. Sound wave velocities in evaporated amorphous Ge films were found to be 76.8% of the directionally averaged crystalline speed.[35] The coefficient of thermal expansion for amorphous Si is 1% smaller than the crystalline value at the average temperature and agrees, within error, with the value of 2.8×10^{-6}/K for implanted Si.[36]

To obtain the value of the biaxial modulus at other temperatures, the dependence of the {100} biaxial modulus on temperature, $d\ln[E/(1-\nu)]/dT$, for the corresponding crystalline materials was used. As $E/(1-\nu)=C_{11}+C_{12}+2C_{12}^2/C_{11}$, its temperature dependence is

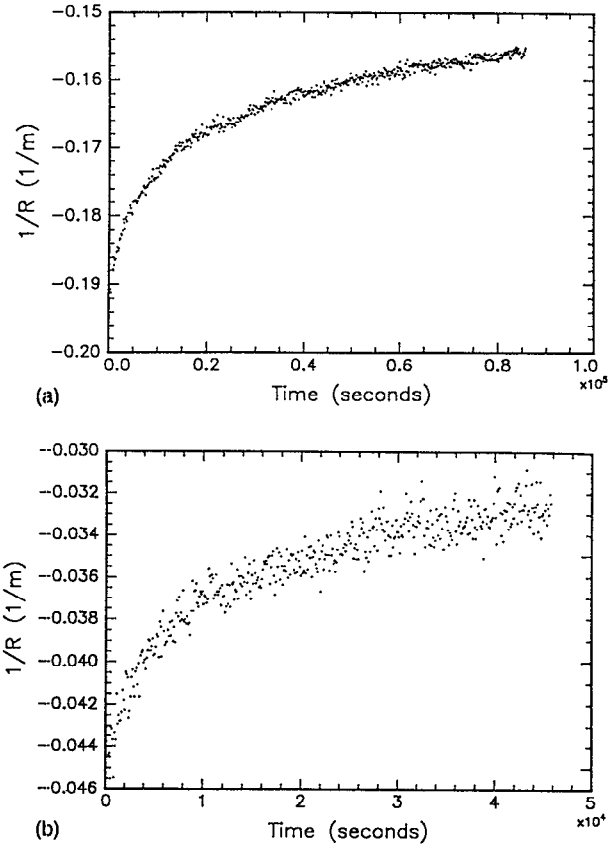

FIG. 1. (a) Stress relaxation of an amorphous Si thin film on a Si(100) substrate under compression at 201 °C. The proportionality constant between curvature $1/R$ and stress σ is equal to 2977 MPa m [Eq. (1)]. (b) Stress relaxation of an amorphous Ge thin film on a Si(100) substrate under compression at 201 °C. The proportionality constant between curvature $1/R$ and stress σ is equal to 3742 MPa m [Eq. (1)].

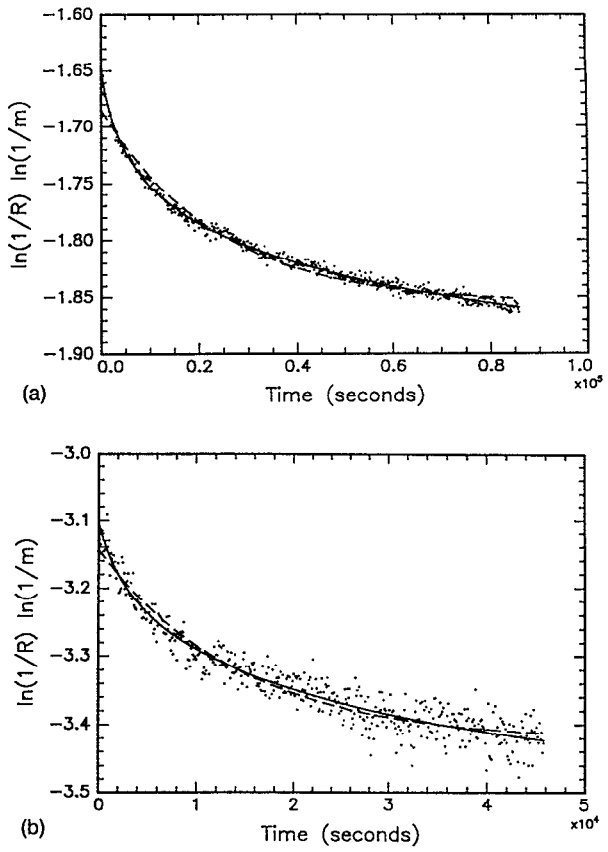

FIG. 2. (a) Logarithmic plot of Fig. 1(a). The data are fitted with a bimolecular (—) and a unimolecular (---) relaxation equation. The fitting parameters for the bimolecular process are: $\ln(1/R_0) = -1.646 \pm 0.001$, $\eta_0 = 6.8\times10^{14} \pm 0.3\times10^{14}$ Pa s, and $\dot{\eta} = 44.4\times10^{10} \pm 0.3\times10^{10}$ Pa ($\chi^2 = 1.1\times10^{-5}$); and for the unimolecular process are: $\ln(1/R_0) = -1.685 \pm 0.001$, $\eta_0 = 3.22\times10^{15} \pm 0.06\times10^{15}$ Pa s, and $k = 4.23\times10^{-5} \pm 0.07\times10^{-5}$/s ($\chi^2 = 4.1\times10^{-5}$). (b) Logarithmic plot of Fig. 1(b). The data are fitted with a bimolecular (—) and a unimolecular (---) relaxation equation. The fitting parameters for the bimolecular process are: $\ln(1/R_0) = -3.101 \pm 0.008$, $\eta_0 = 3.3\times10^{14} \pm 0.4\times10^{14}$ Pa s, and $\dot{\eta} = 21.0\times10^{10} \pm 0.6\times10^{10}$ Pa ($\chi^2 = 3.9\times10^{-4}$); and for the unimolecular process are: $\ln(1/R_0) = -3.143 \pm 0.004$, $\eta_0 = 1.01\times10^{15} \pm 0.04\times10^{15}$ Pa s, and $k = 7.0\times10^{-5} \pm 0.3\times10^{-5}$/s ($\chi^2 = 4.4\times10^{-4}$).

$$-\frac{d\ln[E/(1-\nu)]}{dT} = \frac{C_{11}^2 + C_{12}^2}{C_{11}^2 + C_{11}C_{12} - 2C_{12}^2}\left(-\frac{d\ln C_{11}}{dT}\right) + \frac{C_{11}C_{12} - 4C_{12}^2}{C_{11}^2 + C_{11}C_{12} - 2C_{12}^2}\left(-\frac{d\ln C_{12}}{dT}\right), \tag{4}$$

with C_{ij} the elements of the elastic modulus tensor. Using the literature values for C_{ij} and their change with temperature,[31,32] gives, for {100} Si,

$$\frac{d\ln[E/(1-\nu)]}{dT} = -62\times10^{-6}/\mathrm{K},$$

and for {100} Ge,

$$\frac{d\ln[E/(1-\nu)]}{dT} = -120\times10^{-6}/\mathrm{K}.$$

B. Viscous flow

Figures 1(a) and 1(b) show the results of a stress relaxation experiment on, respectively, a Si and a Ge thin film on a Si(100) substrate at 201 °C. According to Eq. (2) the stress, or the curvature, decreases exponentially if the viscosity is constant. A logarithmic plot [Figs. 2(a) and 2(b)] shows that this is not the case. The viscosity is changing due to structural relaxation. In other covalently bonded amorphous materials, such as silicate glasses, structural relaxation far from metastable equilibrium is manifested by a linear increase in the viscosity with time t: $\eta = \eta_0 + \dot{\eta}t$, with η_0 and $\dot{\eta}$ constants. This is generally interpreted by the biomolecular annihilation of the dangling bonds that govern viscous flow, and whose concentration n is inversely proportional to the viscosity:[37–39] if

$$\frac{dn}{dt} = -k_r n^2, \tag{5a}$$

and

$$\eta = \frac{\eta_0 n_0}{n}, \tag{5b}$$

then

$$\dot{\eta} = \eta_0 n_0 k_r \tag{5c}$$

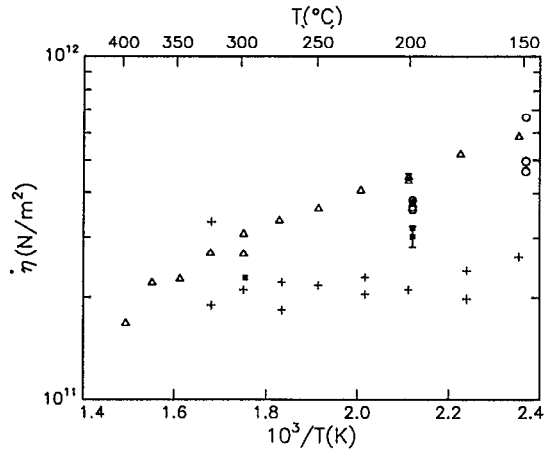

FIG. 3. Rate of viscosity increase as a function of temperature for ion-beam-sputtered amorphous Si [three deposition runs: as1 (△), asi2 (○), and asi3 (■)] and amorphous Ge [age1(+)].

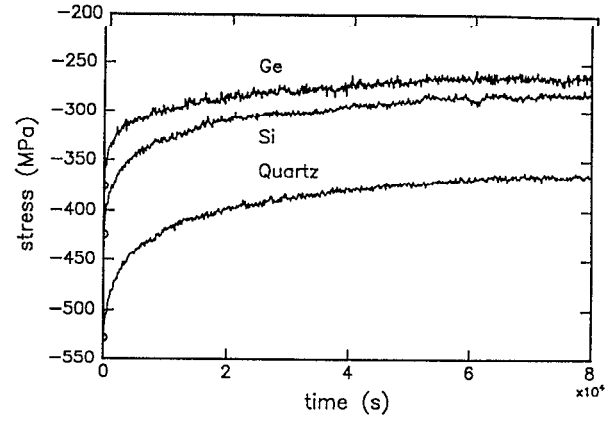

FIG. 4. Stress relaxation in three amorphous Si thin films on a Ge(111) (Ge), a Si(100) (Si), and a fused quartz (Quartz) substrate at 199 °C. The initial stresses in these films are different from those in films deposited on these different substrates at liquid-nitrogen temperature.

is constant, with k_r a constant and n_0 the initial defect concentration.

For a linearly increasing viscosity Eq. (2) has the solution

$$\ln \sigma = \ln \sigma_0 - \frac{E_f}{6(1-\nu_f)\dot{\eta}} \ln\left(1+\frac{\dot{\eta}}{\eta_0}t\right), \tag{6}$$

where σ_0 is the initial stress.

As an alternative the unimolecular annihilation of the flow defects, which results in an exponential decay of their concentration[39] and hence $\eta=\eta_0 \exp(k_r t)$, can be considered. Equation (2) thus gives for the stress relaxation

$$\ln \sigma = \ln \sigma_0 - \frac{E_f}{6(1-\nu_f)\eta_0}[1-\exp(-k_r t)]. \tag{7}$$

A least-squares-fitting routine[40] was used to fit the logarithmic plot [Figs. 2(a) and 2(b)] with both the bimolecular [Eq. (6)] and the unimolecular [Eq. (7)] relaxation models. The bimolecular equation fits the data the best for both materials. The bimolecular relaxation equation was used to fit all other data and the fitting parameter $\dot{\eta}$ for all experiments on samples from three deposition runs for amorphous Si and from one deposition run for amorphous Ge is presented as a function of temperature in Fig. 3. $\dot{\eta}$ increases with decreasing temperature in a non-Arrhenius fashion for amorphous Si and is only very slightly temperature dependent for amorphous Ge.

There is some variation in the value of $\dot{\eta}$ for the different deposition runs of amorphous Si. As can be seen on Fig. 3, the biggest difference is between $\dot{\eta}=44\pm1\times10^{10}$ Pa (asi1) and $30\pm2\times10^{10}$ Pa (asi3) at 201 °C. Measurement errors, arising from calibrations, bare substrate curvature, and fit, cannot explain the difference. Samples from each deposition run were analyzed with the electron microprobe, but no systematic variation in impurity concentration was found. The only measurable impurities were O (about 3.5 at. % in asi1, the oldest samples with the longest anneals, 1 at. % in asi2, and 1.9 at. % in asi3), Ar (about 0.2 at. % in asi1 and asi2 and about 0.3 at. % in asi3), Fe (about 0.1 at. % in asi2 and below the detection limit of 0.01 at. % in the other samples), and Al (very close to the detection limit of 0.004 at. % for all samples). The oxygen is probably predominantly from the surface oxide layer. It should be noted, however, that the relative variations in $\dot{\eta}$ for the different deposition runs of amorphous Si are no larger than those for different samples of the same deposition run of amorphous Ge (Fig. 3).

Since the stress in these amorphous films becomes less compressive during annealing, the possible contribution of densification[36] to the change in substrate curvature needs to be considered; non-Newtonian flow should be considered as well, since the initial stress in the amorphous Si thin films is large. In order to ascertain the Newtonian character of the viscous flow in these films, amorphous Si samples with different initial stresses were prepared by depositing them on three different substrates [Si(100), fused quartz, and Ge(111)] at liquid-nitrogen temperature (deposition run asi3 in Fig. 3). The results of the stress relaxation runs on these three samples at 199 °C are presented in Fig. 4. The curves for the samples on Si(100) and fused quartz were shifted by 167 and 194 s, respectively, to start with the same initial viscosity as the sample on Ge(111): 1.3×10^{14} Pa s. For the viscous flow to be Newtonian the change in stress $\Delta\sigma$ over a fixed time (8×10^4 s), which is equal to the integrated strain rate times the biaxial modulus [see Eq. (2)], should be proportional to the initial stress σ_0. Figure 5 shows that, within the experimental error, this is the case. Another important observation is that the whole relaxation experiment can be fit by a single value of $\dot{\eta}$. The same $\dot{\eta}$ is found if only parts of the relaxation curve are fitted. This observation of a constant $\dot{\eta}$ and the scaling of the stress relaxation with the initial stress independently of elapsed time—and hence the degree of densification—support the entire attribution of the changes of curvature to viscous flow.[6] If densification occurs, its effect is either imperceptibly small or it occurs entirely during the heat-up time between runs.

The isoconfigurational activation enthalpy Q can be

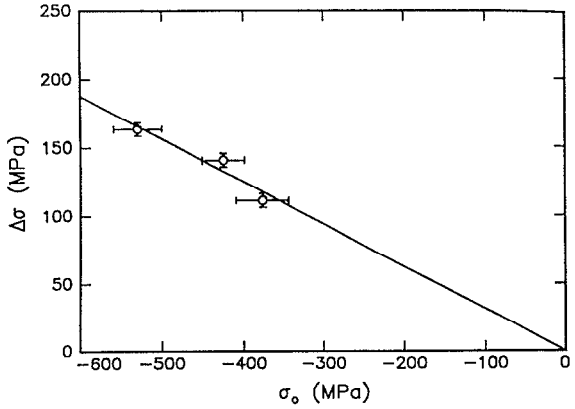

FIG. 5. As required for Newtonian viscous flow, the change in stress over a period of 8×10^4 s is, within error, proportional to the initial stress in the amorphous Si thin films deposited on three different substrates (Fig. 4).

determined by matching calculated and measured viscosity changes during heat up between the viscous flow runs.[25,41] The results for amorphous Si and Ge are presented in Table II. The average activation enthalpy is 1.8 ± 0.3 eV for amorphous Si and 2.6 ± 1.3 eV for amorphous Ge. Most of the data was taken by raising the temperature because the range of viscosities attainable makes that the easiest experiment. However, one data point in Table II(a) was taken during the cooldown from a very short viscous flow run (about 1 h) at 297–247 °C. Due to the high viscosities at 247 °C, only an average viscosity could be determined. For the bimolecular fit of the data at 247 °C, $\dot{\eta}$ was fixed at a value interpolated between 199 and 297 °C using the linear dependence of $\log\dot{\eta}$ vs $1/T$ (Fig. 3), and only η_0 was allowed to vary. The result, $Q=2.135$ eV, lies in the range of values for Q measured during heat up. This shows that the process that changes the isoconfigurational viscosity as a function of temperature is a reversible one.

TABLE II. Isoconfigurational activation enthalpy Q for the viscosity of (a) amorphous Si and (b) amorphous Ge thin films, determined by matching calculated and measured viscosity changes during heat up. η_1 is the viscosity measured at the start of the heat up at temperature T_1 and η_2 is the viscosity measured at the end of the heat up at temperature T_2.

Sample	T_1 (°C)	η_1 (Pa s)	T_2 (°C)	η_2 (Pa s)	Heat-up time (h)	Q (eV)
			(a) Si			
asi1a	201	2.5×10^{16}	298	2.9×10^{14}	0.3475	1.520
	347	1.3×10^{16}	397	6.9×10^{14}	0.2556	2.202
asi1b	176	3.1×10^{16}	225	7.7×10^{14}	0.1694	1.569
	225	1.2×10^{16}	274	3.4×10^{14}	0.1228	1.857
	274	2.0×10^{16}	323	6.2×10^{14}	0.2767	2.107
	323	7.4×10^{15}	372	5.0×10^{14}	0.2981	2.023
asi1f	152	4.1×10^{16}	201	6.8×10^{14}	0.1311	1.535
	201	3.9×10^{16}	249	6.9×10^{14}	0.1239	1.824
	249	3.2×10^{16}	298	9.0×10^{14}	0.2439	1.940
asi2a	149	2.3×10^{16}	199	2.6×10^{14}	0.1550	1.952
asi2c	149	1.7×10^{16}	199	3.2×10^{14}	0.1839	1.538
asi2d	149	1.7×10^{16}	199	3.6×10^{14}	0.1914	1.528
asi3a	199	2.5×10^{16}	247	6.3×10^{14}	0.1478	1.656
	247	1.5×10^{15}	297	7.0×10^{13}	0.1397	2.165
	297	8.9×10^{14}	247	5.8×10^{16}	0.1361	2.135
			(b) Ge			
agea	152	1.6×10^{16}	201	3.3×10^{14}	0.1778	1.476
	201	9.9×10^{15}	249	1.8×10^{14}	0.1128	1.883
	249	8.6×10^{15}	298	4.4×10^{14}	0.1950	1.707
agec	124	1.9×10^{16}	174	1.2×10^{14}	0.0889	1.632
	174	7.5×10^{15}	223	7.3×10^{13}	0.1506	2.956
	223	1.2×10^{16}	272	1.8×10^{14}	0.3445	2.403
	272	9.0×10^{15}	322	1.0×10^{14}	0.3161	5.741
aged	174	1.2×10^{16}	223	1.3×10^{14}	0.2131	2.089
	223	2.2×10^{16}	272	1.9×10^{14}	0.3608	3.515
	272	1.1×10^{16}	322	1.1×10^{14}	0.2097	2.968

IV. DISCUSSION

A detailed atomistic model for viscous flow of a covalent random network still needs to be developed. The observation of bimolecular structural relaxation kinetics suggests that the rearrangement governing flow needs the presence of a pre-existing dangling bond, or of any other defect that anneals out bimolecularly. If it is assumed that the defect motion has a single activation enthalpy ($Q=1.8$ eV), viscosities measured at different temperatures can be compared isothermally. For example, extrapolation of the as-deposited viscosity of one of the samples (e.g., 7.4×10^{14} Pa s at 152 °C for asi1f) to 298 °C gives a value that is seven orders of magnitude higher than the measured final viscosity (2.4×10^{16} Pa s) for that sample at 298 °C. The simplest interpretation is that the defect concentration decreased by the same factor [Eq. 5(b)]. A spread in the values of the activation enthalpies or a certain degree of nonisoconfigurationality of the experiments may change this interpretation. The number of neutral dangling bonds in these samples was measured by electron paramagnetic resonance (EPR) (Table III),[42] and the concentration of neutral dangling bonds after all anneals was found to decrease by only a factor of 6. Therefore, it seems unlikely that the defects that govern viscous flow are indeed neutral dangling bonds. However, as differential scanning calorimetry (DSC) experiments have shown,[9,10,16] EPR only measures a very small portion of the defects in amorphous Si. Other defects could be involved in the viscous flow process, such as charged dangling bonds, which anneal out bimolecularly with dangling bonds of opposite charge, or vacancies (four dangling bonds together), which anneal out bimolecularly with interstitials.

The value of the average isoconfigurational activation enthalpy for the viscosity, 1.8 eV, is close to the strength of a Si—Si bond according to Pauling.[43] It should be kept in mind that there is no unanimity on the exact value of the bond strength; for example, the value based on the cohesive energy is 2.32 eV.[44,45] It can therefore be assumed that the activation enthalpy corresponds to the breaking of an additional Si—Si bond, possibly a strained one, which may provide the freedom necessary for the flow defect to rear-

TABLE III. The number of neutral dangling bonds in the as-deposited and annealed amorphous Si samples asi1.

Sample	Highest temperature (°C)	Ending viscosity (extrapolated to 298 °C with $Q=1.8$ eV) (Pa s)	Neutral dangling bond density ($/cm^3$)
asi1d	as deposited	2.6×10^{9}	1.9×10^{19}
asi1a	397	1.1×10^{18}	1.8×10^{18}
asi1b	372	9.7×10^{17}	3.0×10^{18}
asi1f	298	2.4×10^{16}	3.2×10^{18}

range so as to produce local shear. Figure 6 shows an atomistic picture of how flow might occur. Flow could be easier if the flow defect were formed near a positively charged dangling bond, which attracts the electrons of the neighboring bond even in the absence of a stress.

A little more information can be obtained by comparing the present results with those from DSC on amorphous Si.[9–11,16,18] DSC scans at 40 K/min of implanted[9–11,16,18] or ion-beam-sputtered[46] amorphous Si shows an almost uniform exothermic release of about 7 W/mol due to structural relaxation at all temperatures below the crystallization peak. This has been interpreted as structural relaxation governed by processes with a wide spectrum of activation enthalpies.[11,18] Isothermal runs can be modeled by bimolecular relaxation of the defects. The recombination constant k_r [Eq. (5a)] is almost independent of temperature.[18] This is very different for the k_r found for the bimolecular annihilation of the flow defects. Since the isoconfigurational activation enthalpy for flow Q is 1.8 eV and the average activation enthalpy for $\dot{\eta}$ is about 0.1 eV (Fig. 3), Eq. (5c) shows that, if the defect concentration n is constant during an isoconfigurational experiment, the temperature dependence of the recombination constant for flow defects is

$$k_r(T)=k_{r0}\exp(-Q_r/kT), \tag{8}$$

with $Q_r=1.7$ eV. Their difference can be explained, for example, if the flow defects are just a fraction of the defects that give off heat during the DSC scan. A calculation of the DSC signal, dH/dt, with constant scan rate $b=dT/dt$ arising from just the annihilation of the flow defects illustrates this point:

$$\frac{dH}{dt}=-H_0\frac{dn}{dt}=-H_0 b\frac{dn}{dT}. \tag{9}$$

H_0 is the heat released when one defect is annihilated. Using Eqs. (5a) and (6), $dT=b\,dt$, and the assumption $Q_r\gg k_BT$ to simplify the exponential integral in the calculations[47] gives

$$\frac{dn}{dT}=-\frac{k_r(T)}{b}\times\frac{(2k_BT/Q_r+1)}{(1/n_0)+(k_B/bQ_r)[T^2k_r(T)-T_0^2k_r(T_0)]^2}, \tag{10}$$

with n_0 the initial defect concentration at T_0, the starting temperature of the scan. Figure 7 shows the result for $H_0=0.9$ eV (half the Si—Si bond energy[43]), $k_{r0}=10^{12}/s$ (typical attempt frequency; a typical atomic vibration frequency is $10^{12}/s$; the entropy factors associated with the activation process may raise this value somewhat, but this effect is usually negligible[44]), $Q_r=1.7$ eV, and $b=40$ K/min and a series of initial concentrations n_0 at $T_0=300$ K. The peak becomes broader and shifts to higher temperatures for lower defect concentrations. As the maximum DSC signal has to be smaller than 7 W/mol, the upper bound for the initial concentration of flow defects is 1.2% or $6\times10^{20}/cm^3$, which gives a peak at 729 K. The maximum heat release from all the flow defects is only about one-fifth of the total heat release from structural relaxation (5 kJ/mol) seen in the DSC.

The macroscopic viscosity η can be written in terms of the dimensions and the motion of the defects that govern it as[48]

$$\eta=\frac{k_BT}{(\gamma_0V_0)^2nk_f}, \tag{11}$$

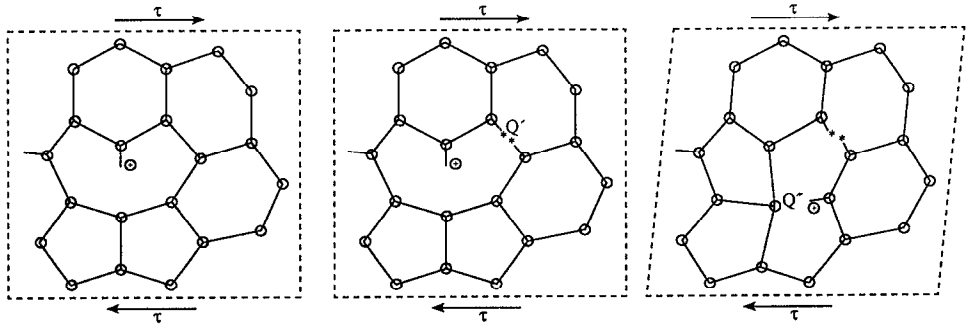

FIG. 6. Schematic diagram of a possible mechanism for viscous flow of amorphous silicon (see also Fig. 8). (a) The initial state of the flow defect is a charged dangling bond. (b) A nearby bond is broken thermally with an activation enthalpy Q'. (c) The flow jump: A dangling bond connects with a nearby atom, thereby creating a new dangling bond and local shear γ_0 (activation enthalpy Q''). This results in macroscopic shear (dashed line) and an amount of work $\tau\gamma_0V_0$ done by the external shear stress τ. The flow jump (c) repeats until two dangling bonds recombine.

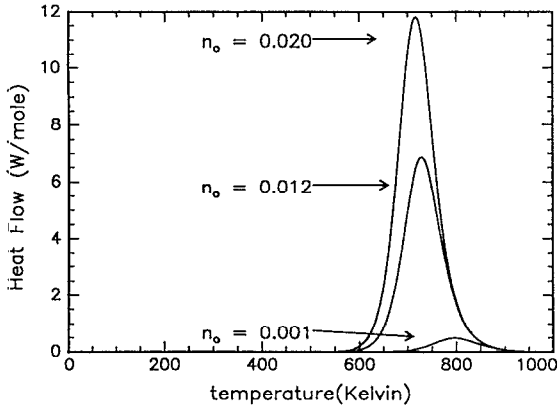

FIG. 7. Calculated heat flow in a DSC scan with a scanning rate of 40 K/min for the bimolecular annihilation of the flow defects for three different initial defect concentrations n_0.

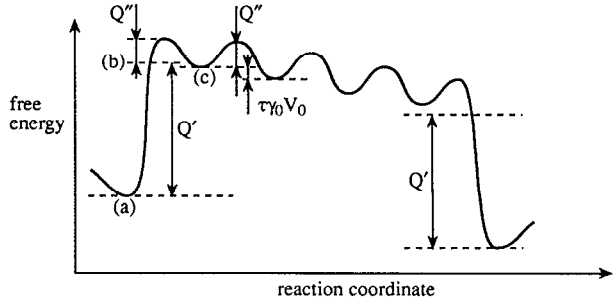

FIG. 8. Schematic diagram of the free energy changes as a function of the reaction coordinate for a viscous flow processes that occurs by a chain reaction. The letters correspond to the configurations of Fig. 6. Q' is the free energy needed to activate the flow defect: Q'' is the free energy needed to make a flow jump; the total activation enthalpy is $Q=Q'+Q''$. With each flow jump the free energy of the system is lowered by $\tau\gamma_0 V_0$, the work done by the applied stress. In this diagram the flow defect makes five jumps before two dangling bonds recombine.

where V_0 is the volume of the rearranging region (defect), γ_0 the shear strain of the rearrangement, and $k_f = k_0 \exp(-Q/kT)$ is the rearrangement frequency. Equation (11) may be used to estimate some limitations on the nature of the defects. For an as-deposited film η was found to be 7.4×10^{14} Pa s at $T=152$ °C. Taking $k_0=10^{12}$/s, a typical attempt frequency, and $Q=1.8$ eV gives $k_f=5\times10^{-10}$/s. Since clearly $n<1/\Omega$, with Ω the atomic volume, it follows from Eq. (10) that $(\gamma_0 V_0)>28\ \Omega$. Structural models, such as Fig. 6, indicate that $\gamma_0 V_0$ is probably less than Ω. The viscosity of the amorphous Si is thus much lower than expected from this model. A similar problem was encountered for the crystallization of Si by single-phase-epitaxy growth, where the growth rates have an anomalously high prefactor.[44] This was interpreted by assuming that one activation step leads to a chain reaction.[49] This interpretation could be valid here as well: One activation step can lead to several bond rearrangements in the loosened network structure around the defect before the newly broken bonds recombine.

If plastic flow happens by a chain reaction, Eq. (11) needs to be reevaluated. The arguments of Ref. 48 thus give a shear strain rate $\dot{\gamma}$,

$$\dot{\gamma}=n\exp\left(\frac{-Q'}{kT}\right)\sum_1^N k_0\exp\left(-\frac{Q''}{kT}\right)\beta(\tau)\gamma_0 V_0 \qquad (12)$$

where $Q'+Q''=Q$ and $n\exp(-Q'/kT)$ is the number of flow defects in the activated state (additional broken bond nearby), N is the total number of jumps of the flow defect for one activation step, and $k_0\exp(-Q''/kT)\beta(\tau)$ the net jump frequency of a flow defect in the activated state under the action of the stress. $\beta(\tau)$ reflects the biasing of the jumps in the forward direction due to the applied stress. Simple rate theory gives[50]

$$\beta(\tau)=\sinh\left(\frac{\tau\gamma_0 V_0}{kT}\right), \qquad (13)$$

where $\tau\gamma_0 V_0$, the work done by the applied stress, is the difference in chemical potential between the forward and the backward positions for one jump of the flow defect (Fig. 8). For small stresses this gives the equivalent of Eq. (11),

$$\eta=\frac{\tau}{\dot{\gamma}}=\frac{k_B T}{N(\gamma_0 V_0)^2 n k_f}. \qquad (14)$$

Equation (14) can yield low viscosities even if $\gamma_0 V_0$ is, as expected, smaller than Ω.

Such unexpectedly low viscosity values are seen in metallic glasses as well[51–53] and it is possible that the origin of the problem is the same for all amorphous materials. Therefore, the approaches taken in the literature to solve the problem for amorphous metals are examined for possible application to amorphous Si.

Berry proposed a temperature-dependent activation energy.[54] In order to explain the low viscosities, however, the activation enthalpy should become smaller with temperature, which is contrary to the observations for metallic glasses[55] as well as for the data obtained here (Table II).

Another suggestion was reversible changes in the flow defect concentration of metallic glasses with temperature.[48,51,53,55] Unlike the defects in metallic glasses, which can be thought of as free volume fluctuations, dangling bonds are probably not created by changes in volume due to thermal expansion. They can be created reversibly at high temperature in any structural state due to the rise in configurational entropy, just like the equilibrium defects in a crystalline structure. The number of these "equilibrium" defects is very small [$\sim\exp(-0.9\ \text{eV}/kT)$], but under some conditions their contribution to the flow process and its isoconfigurational activation enthalpy might be important. They can probably not account for the observed low viscosities, since the number of nonequilibrium defects has to be small in order for the thermally activated defects to play a role, but they might explain the apparent increase in the isoconfigurational activation enthalpy with increasing temperature [Table II(a)].

V. CONCLUSION

The biaxial modulus Y and coefficient of thermal expansion α of ion-beam-sputtered amorphous Si and Ge thin films were determined from stress versus temperature measurements on samples deposited on Si(100) and fused quartz substrates. For amorphous Si, at the average temperature of 110 °C, $Y=14\pm1\times10^{10}$ Pa and $\alpha=3.0\pm0.3\times10^{-6}$/K and for amorphous Ge, at the average temperature of 172 °C, $Y=12\pm1\times10^{10}$ Pa and $\alpha=7.9\pm0.7\times10^{-6}$/K.

Newtonian viscous flow, its temperature dependence, and its change with time due to structural relaxation has been observed for the first time for amorphous Si and Ge. The data can be best fitted with a viscosity that increases linearly with time, characteristic of a bimolecular flow defect annihilation process. The isoconfigurational activation enthalpy for the viscosity is 1.8 ± 0.3 eV for amorphous Si and 2.6 ± 1.3 eV for amorphous Ge. The value for amorphous Si together with the lower than expected viscosities, suggests that the critical activation step for flow is the breaking of an additional Si—Si bond and that several flow jumps of the defect occur before these newly broken bonds recombine.

ACKNOWLEDGMENTS

We thank M. J. Aziz, G. Q. Lu, C. A. Volkert, and S. Roorda for useful discussions, A. V. Wagner for the preparation of the Si sputtering target, S. Coffa for the EPR measurements, and D. Lange for the electron microprobe analysis of the samples. This work has been supported by the Office of Naval Research under Contract No. N00014-91-J-1281 and by the NSF through the Harvard Materials Research Laboratory under Contract No. DMR-89-20490. A.W. acknowledges support by a predoctoral fellowship from IBM.

[1] D. E. Polk, J. Non-Cryst. Solids **13**, 153 (1973).
[2] G. A. N. Connell and R. J. Temkin, Phys. Rev. B **12**, 5323 (1974).
[3] P. Steinhardt, R. Alben, and D. Weaire, J. Non-Cryst. Solids **15**, 199 (1974).
[4] P. A. Flinn, D. S. Gardner, and W. D. Nix, IEEE Trans. Electron Devices **ED-34**, 689 (1987).
[5] A. Witvrouw and F. Spaepen, Mater. Res. Soc. Symp. Proc. **188**, 147 (1990).
[6] A. Witvrouw and F. Spaepen, Mater. Res. Soc. Symp. Proc. **205**, 21 (1992). The values of $\dot{\eta}$ and η_0 for *a*-Si in the present article are slightly different from those in Ref. 6 due to an improved calibration procedure and the use of the measured biaxial modulus instead of a literature value.
[7] A. Witvrouw, C. A. Volkert, and F. Spaepen, Mater. Sci. Eng. A **134**, 1274 (1991).
[8] C. A. Volkert, Mater. Res. Soc. Symp. Proc. **157**, 635 (1990); J. Appl. Phys. **70**, 3521 (1991).
[9] S. Roorda, Ph.D. thesis, Rijksuniversiteit te Utrecht, The Netherlands, 1990.
[10] S. Roorda, S. Doorn, W. C. Sinke, P. M. L. O. Scholte, and E. van Loenen, Phys. Rev. Lett. **62**, 1880 (1989).
[11] E. P. Donovan, F. Spaepen, J. M. Poate, and D. C. Jacobson, Appl. Phys. Lett. **55**, 1516 (1989).
[12] B. Park, Ph.D. thesis, Harvard University, 1989.
[13] W. C. Sinke, S. Roorda, and F. Saris, J. Mater. Res. **3**, 1201 (1988).
[14] G. K. Hubler, E. P. Donovan, K. W. Wang, and W. G. Spitzer, SPIE **350**, 220 (1985).
[15] E. P. Donovan, G. K. Hubler, and C. N. Wadell, Nucl. Instrum. Methods B **19**, 590 (1987).
[16] S. Roorda, J. M. Poate, D. C. Jacobson, D. J. Eaglesham, B. S. Dennis, S. Dierker, W. C. Sinke, and F. Spaepen, Solid State Commun. **75**, 197 (1990).
[17] S. Roorda, W. C. Sinke, J. M. Poate, D. C. Jacobson, S. Dierker, B. S. Dennis, D. J. Eaglesham, and F. Spaepen, Mater. Res. Soc. Symp. Proc. **157**, 683 (1990).
[18] S. Roorda, W. C. Sinke, J. M. Poate, D. C. Jacobson, S. Dierker, B. S. Dennis, D. J. Eaglesham, F. Spaepen, and P. Fuoss, Phys. Rev. B **44**, 3702 (1991).
[19] G. W. Scherer, *Relaxation in Glass and Composites* (Wiley, New York, 1986), p. 149.
[20] R. Bhadra, J. Pearson, P. Okamoto, L. Rehn, and M. Grimsditch, Phys. Rev. B **38**, 12656 (1988).
[21] X. Jiang, B. Goranchev, K. Schmidt, P. Grünberg, and K. Reichelt, J. Appl. Phys. **67**, 6772 (1990).
[22] F. Jansen and M. A. Machonkin, J. Vac. Sci. Technol. A **6**, 1696 (1988).
[23] W. D. Nix, Metall. Trans. A **20**, 2217 (1989).
[24] M. F. Doerner and W. D. Nix, CRC Crit. Rev. Solid State Mater. Sci. **14**, 225 (1988).
[25] A. Witvrouw and F. Spaepen (unpublished).
[26] F. Jansen and M. A. Machonkin, J. Vac. Sci. Technol. A **6**, 1696 (1988).
[27] R. W. Hoffman, Mater. Res. Soc. Symp. Proc. **130**, 295 (1989).
[28] A. Witvrouw and F. Spaepen, J. Appl. Phys. **73**, 7344 (1993).
[29] F. Spaepen, A. L. Greer, K. F. Kelton, and J. L. Bell, Rev. Sci. Instrum. **56**, 1340 (1985).
[30] J. S. Custer, M. O. Thompson, D. C. Jacobson, J. M. Poate, S. Roorda, W. C. Sinke, and F. Spaepen, Mater. Res. Soc. Symp. Proc. **157**, 689 (1990).
[31] W. A. Brantley, J. Appl. Phys. **44**, 534 (1973).
[32] H. B. Huntington, in *Solid State Physics*, edited by F. Seitz and D. Turnbull (Academic, New York, 1958), Vol. 7, p. 322.
[33] Heraeus catalog, fused quartz and fused silica for optics (Herasil Amersil, Inc., Buford, GA).
[34] C. A. Swenson, J. Phys. Chem. Ref. Data **12**, 179 (1983).
[35] I. R. Cox-Smith, H. C. Liang, and R. O. Dillon, J. Vac. Sci. Technol. A **3**, 674 (1985).
[36] C. A. Volkert, Mater. Res. Soc. Symp. F, Boston, December 1990.
[37] G. J. Roberts and J. P. Roberts, 7th International Conference on Glass, 1965, p. 31.
[38] H. R. Lillie, J. Am. Ceram. Soc. **16**, 619 (1933).
[39] S. S. Tsao and F. Spaepen, Acta Metall. **33**, 881 (1985).
[40] GENPLOT program from Computer Graphics Service.
[41] A. Witvrouw, Ph.D. thesis, Harvard University, 1992.
[42] S. Coffa, AT&T Laboratories (private communication).
[43] L. Pauling, *The Nature of the Chemical Bond*, 3rd ed. (Cornell University Press, Ithaca, NY, 1960), p. 85.
[44] G. Lu, E. Nygren, and M. J. Aziz, J. Appl. Phys. **70**, 5323 (1991).
[45] C. Kittel, *Introduction to Solid State Physics*, 6th ed. (Wiley, New York, 1986), p. 55.
[46] H. Zolla, Harvard University (private communication).
[47] H. Abramowitz and I. E. Stegun, *Handbook of Mathematical Functions* (Dover, New York, 1968), p. 231.
[48] F. Spaepen, in *Physics of Defects*, Les Houches Lectures XXXV, edited by R. Balian *et al.* (North-Holland, Amsterdam, 1981), p. 154.
[49] F. Spaepen and D. Turnbull, AIP Conf. Proc. **50**, 73 (1979).
[50] S. Glasstone, K. J. Laidler, and H. Eyring, in *The Theory of Rate Processes* (McGraw-Hill, New York, 1941), p. 480.
[51] A. I. Taub and F. Spaepen, Acta Metall. **28**, 1781 (1980).
[52] A. van den Beukel, E. Huizer, A. L. Mulder, and S. van der Zwaag, Acta Metall. **34**, 483 (1986).
[53] C. A. Volkert, Ph.D. thesis, Harvard University, 1988.
[54] B. S. Berry, Scr. Met. **16**, 1407 (1982).
[55] S. S. Tsao and F. Spaepen, Acta Metall. **33**, 891 (1985).